[*Electronic Supplementary Information (ESI)*]

Shaping monodispersed azo molecular glass microspheres with polarized light

Hao Huang,[a] Yechao Su,[b] Xinran Zhou,[a] Chuyi Liao,[a] Chungen Hsu,[a] Yi Du,[a] Jianhong Xu*[b] and Xiaogong Wang*[a]

a. Department of Chemical Engineering, Laboratory of Advanced Materials (MOE), Tsinghua University, Beijing, 100084, People's Republic of China.
E-mail: wxg-dce@mail.tsinghua.edu.cn

b. Department of Chemical Engineering, The State Key Lab of Chemical Engineering, Tsinghua University, Beijing, 100084, People's Republic of China.
E-mail: xujianhong@mail.tsinghua.edu.cn

1. ^{1}H NMR spectra of IAC-4 and intermediates for its synthesis

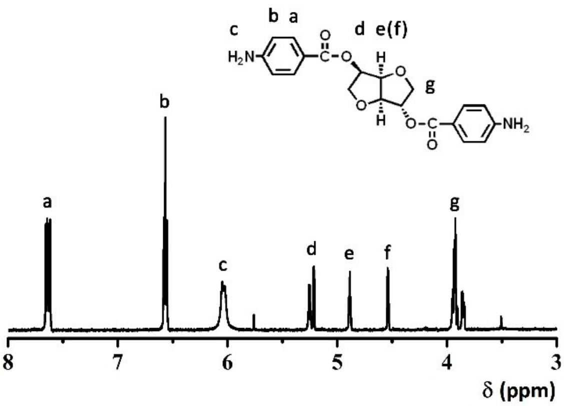

Fig. S1 ^{1}H NMR spectrum of isosorbide *bis*(4-aminobenzoat).

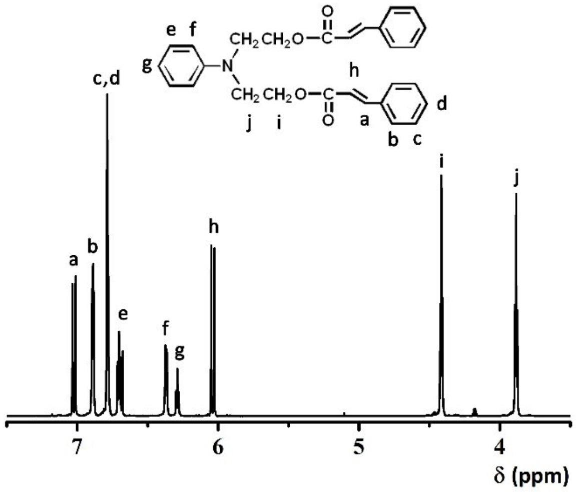

Fig. S2 ^{1}H NMR spectrum of *di*(hydroxyethyl)aniline *bis*cinnamate.

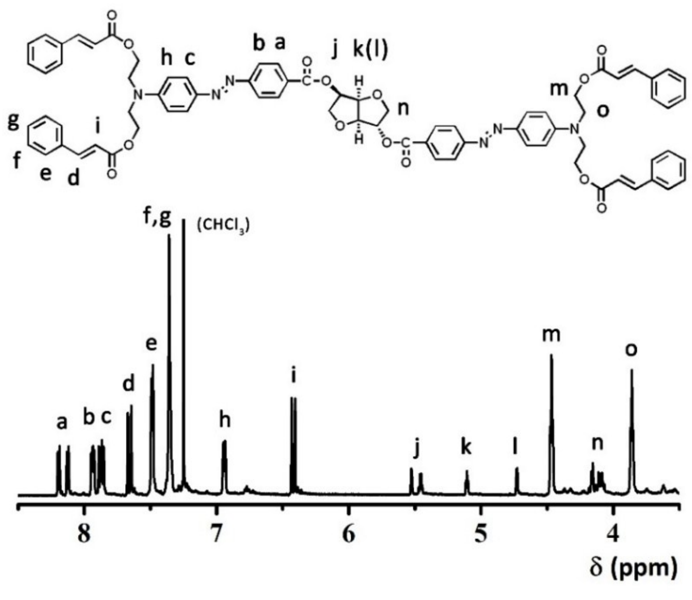

Fig. S3 ^{1}H NMR spectrum of the azo molecular glass (IAC-4).

2. SEM and OM images of the monodispersed IAC-4 microspheres

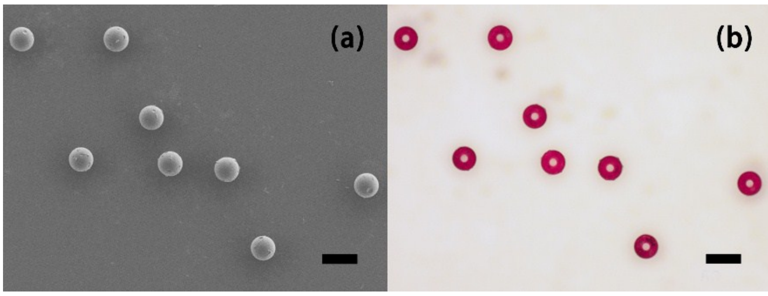

Fig. S4. (a) SEM image, (b) reflection-mode OM image of the monodispersed IAC-4 microspheres with the monodispersed diameter of 14-μm prepared by the microfluidics. These two images are captured from the same region on the silicon substrate to verify the equality of SEM and OM characterization. The scale bars are 20 μm. The centric white spots in the microspheres in Fig. S4b result from the specular reflection of the OM illumination light on the spherical surface of the microspheres and the limited collecting angle of the objective lens in the optical microscope.

3. The laser irradiation set-up for photoinduced deformation

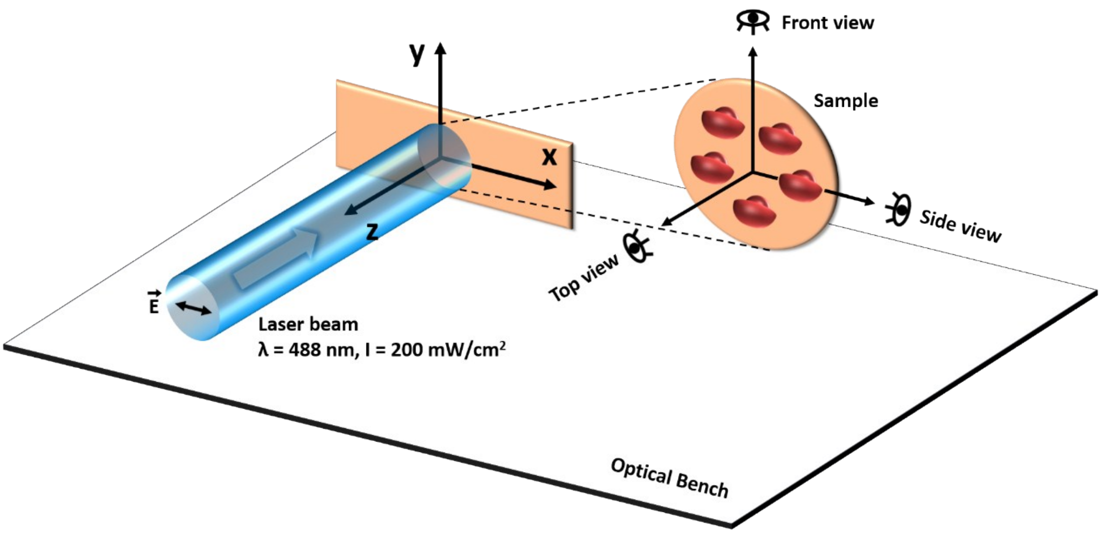

Fig. S5. Schematic illustration of the laser irradiation set-up for studying photoinduced deformation of the microspheres. The Cartesian coordinate system and the definition of the three views (top view, front view and side view) are the same as those given in Fig. 2a. In experiments, the silicon wafer containing the IAC-4 microspheres was vertically settled on the optical bench; the laser beam propagated in the horizontal direction and was perpendicularly incident onto the silicon wafer containing the samples. Thus, in the coordinate system, the laser beam propagated along the negative z-axis, the gravity pointed to the negative y-axis, and the direction of the electric vibration of the incident light was parallel to the x-axis.

4. Bottom-view SEM images of the mushroom-like IAC-4 microparticles

In order to investigate the morphology of the upper cap in detail, SEM images from the bottom view (in the opposite direction of the top view) were also captured. The sample preparation for bottom view observation is schematically illustrated in Fig. S6a. In brief, a silicon wafer covered with a layer of carbon conductive tape was gently pasted onto the silicon wafer that is loaded with the mushroom-like microparticles. No external pressure is applied to the twin silicon wafers in the process. After holding on for 5 min, the upper silicon wafer was peeled off and turned over, during which most of the mushroom-like microparticles were stuck on the carbon conductive tape and detached from the original silicon wafer. Since the physical interaction between the microparticles and the original substrate is much weaker compared with the one between the microparticles and sticky tape, the transferring process almost has no effect on the shape and architecture of the mushroom-like microparticles. Finally, after irradiation with the linearly polarized light for 1.5 h, the morphology of the mushroom-like microparticles on a plane SEM stage was characterized and is shown in Fig. S6b. To provide a more visualized picture of the upper cap, the bottom view SEM image was also captured from a tilting angle of 25°, as shown in Fig. S6c.

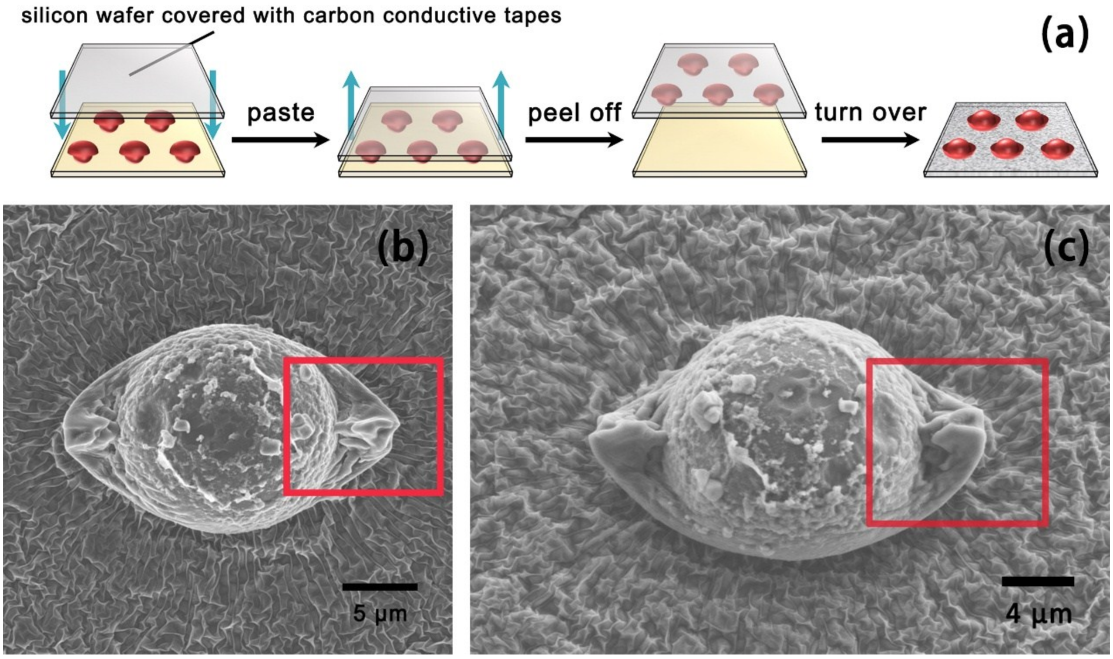

Fig. S6 (a) Schematic illustration of the sample preparation for the bottom view observation. (b) The bottom view SEM image of the mushroom-like IAC-4 microparticles by the linearly polarized light irradiation (λ = 488 nm, I = 200 mW/cm^2) for 1.5 h. (c) The bottom view SEM image with a tilting angle to be 25°. The mushroom-like IAC-4 microparticles were irradiated by the linearly polarized light (λ = 488 nm, I = 200 mW/cm^2) for 1.5 h. The rough and folded background in Fig. S5b and c is the morphology of the carbon conductive tape.

The red frames in Fig. S6b and S6c correspond to the tip of the upper caps, which obviously exhibit a thick ridge in the middle part. This thick ridge is originated from the relatively larger electric field component along z-axis in this region and thus larger deformation degree toward the substrate. In addition, as shown in Fig. 2g, the thick ridge of the downward tip can also be observed from the front view.

5. Calculation of the light refraction in the IAC-4 microspheres

According to the Snell's law,[s1]

$$n_1 \sin(i_1) = n_2 \sin(i_2) \qquad \text{(S1)}$$

when the light is slantwise incident to the interface that separates two isotropic dielectric media with refractive index of n_1 and n_2 (see Fig. S7), the unit propagation vector of the refracted light ($\mathbf{k}_2$) is deviated from that of the incident light ($\mathbf{k}_1$).

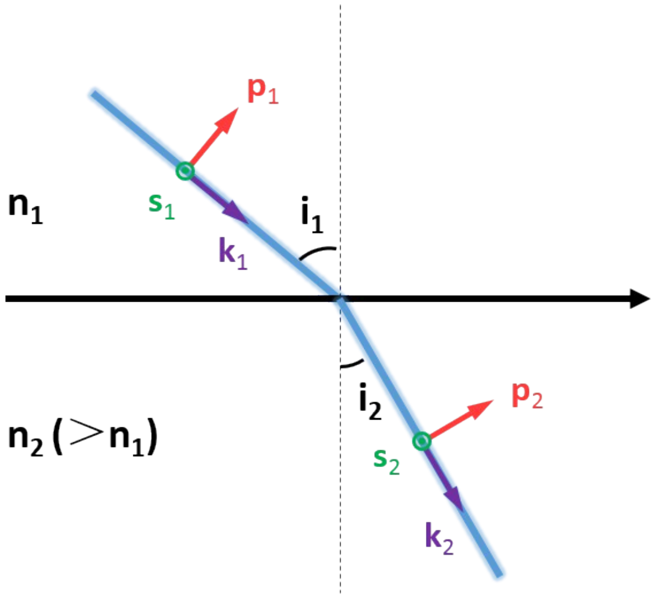

Fig. S7 Schematic illustration of the light refraction on the interface of two dielectric media (refraction index to be n_1 and n_2). i_1 and i_2 are the incident angle and the refracted angle, respectively. **k** is the unit propagation vector representing the light propogation direction. **s** and **p** represent the two orthogonal directions (unit vectors) of the electric field, where **s** is perpendicular to the incident plane and **p** is defined as $\mathbf{p} = \mathbf{s} \times \mathbf{k}$. The subscript 1 and 2 refers to the variables belonging to the media n_1 and n_2, respectively.

According to the Fresnel equations,[s1] the electric field amplitudes of the incident light and refracted light follow the relationship,

$$E_{2p} = \frac{2n_1 \cos(i_1)}{n_2 \cos(i_1) + n_1 \cos(i_2)} E_{1p} \qquad \text{(S2)}$$

$$E_{2s} = \frac{2n_1 \cos(i_1)}{n_1 \cos(i_1) + n_2 \cos(i_2)} E_{1s} \qquad \text{(S3)}$$

where the subscripts **s** and **p** refer to the two orthogonal directions of electric field as shown in Fig. S7; the subscripts 1 and 2 respectively refer to the media with the refraction index of n_1 and n_2.

The calculation about the light refraction in the upper parts of the IAC-4 microsphere is conducted as follows. The refractive index of 1.95 (at 488 nm, measured by ellipsometry) is used for IAC-4. The radius (r) of the IAC-4 microspheres is 7 μm. As shown in Fig. S8, the incident linearly polarized beam propagates along the negative z-axis and its electric field vector (**E**$_1$) is in the x-axis. The linearly polarized light is incident to an arbitrary point A(x, y, z) on the spherical surface, whose azimuth angle and the zenith angle are φ and θ, respectively. The relation between the Cartesian coordinate and the spherical coordinate is,

$$x = r\sin(\theta)\cos(\varphi) \tag{S4}$$

$$y = r\sin(\theta)\sin(\varphi) \tag{S5}$$

$$z = r\cos(\theta) \tag{S6}$$

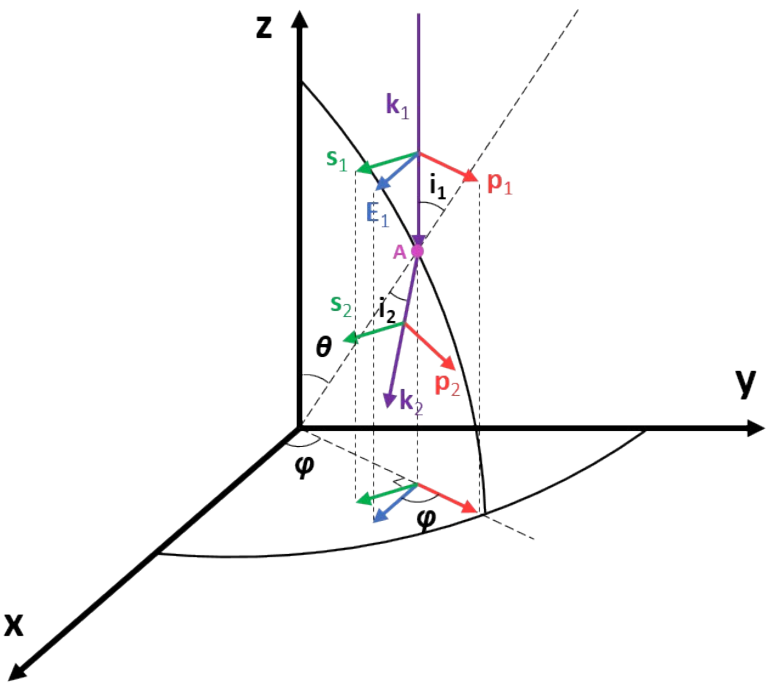

Fig. S8 Schematic illustration of the light refraction in the upper part of the IAC-4 microsphere. The unit propagation vector of the incident light is paralell to the z-axis in the negative direction, with its electric field vector (**E**$_1$) in x-axis direction. φ and θ are respectively the azimuth angle and the zenith angle at the light incident point (A) on the spherical surface. The definition of other variables can consult Fig. S7.

According to the above definition, **k** is the unit propagation vector representing the light propagation direction, **s** is the unit vector perpendicular to the incident plane and

p is defined as **p** = **s** × **k**. Thus, the unit propagation vector of the incident light ($\mathbf{k}_1$) and its electric field component direction ($\mathbf{s}_1$ and $\mathbf{p}_1$) are,

$$\mathbf{k}_1 = (0,0,-1) \tag{S7}$$

$$\mathbf{s}_1 = (\sin\varphi,-\cos\varphi,0) \tag{S8}$$

$$\mathbf{p}_1 = (\cos\varphi,\sin\varphi,0) \tag{S9}$$

The incident angle (i_1) at any region on the surface of the microsphere is equal to its zenith angle (θ). And the electric field vector of the linearly polarized incident light can be expressed by,

$$\mathbf{E}_1 = E_1(1,0,0) \tag{S10}$$

where E_1 is the electric wave amplitude of the incident light. $\mathbf{E}_1$ can be decomposed into the **s** direction and **p** direction,

$$E_{1s} = \mathbf{E}_1 \cdot \mathbf{s}_1 = E_1 \sin\varphi \tag{S11}$$

$$E_{1p} = \mathbf{E}_1 \cdot \mathbf{p}_1 = E_1 \cos\varphi \tag{S12}$$

According to the Snell's Law, the refracted angle i_2 is,

$$i_2 = \arcsin(n_1 / n_2 \cdot \sin(i_1)) \tag{S13}$$

The unit propagation vector of the refracted light ($\mathbf{k}_2$) and its electric field components ($\mathbf{s}_2$ and $\mathbf{p}_2$) are,

$$\mathbf{k}_2 = (\sin(i_1\text{-}i_2)\cdot\cos\varphi,\sin(i_1\text{-}i_2)\cdot\sin\varphi,\cos(i_1\text{-}i_2)) \tag{S14}$$

$$\mathbf{s}_2 = \mathbf{s}_1=(\sin\varphi,-\cos\varphi,0) \tag{S15}$$

$$\mathbf{p}_2 = \mathbf{s}_2 \times \mathbf{k}_2 = (-\cos(i_1\text{-}i_2)\cdot\cos\varphi,-\cos(i_1\text{-}i_2)\cdot\sin\varphi,\sin(i_1\text{-}i_2)) \tag{S16}$$

According to the Fresnel equations,

$$E_{2s} = \frac{2n_1\cos(i_1)}{n_1\cos(i_1)+n_2\cos(i_2)}E_{1s} \tag{S17}$$

$$E_{2p} = \frac{2n_1\cos(i_1)}{n_2\cos(i_1)+n_1\cos(i_2)}E_{1p} \tag{S18}$$

Finally, the electric field vector of the refracted light ($\mathbf{E}_2$) can be obtained,

$$\mathbf{E}_2 = E_{2s}\mathbf{s}_2 + E_{2p}\mathbf{p}_2 \tag{S19}$$

The calculation results for the linearly polarized light irradiation are shown in Fig. 5 and Fig. S9. For the circularly polarized light irradiation, there is a relative phase difference of $\pi/2$ between $\mathbf{E}_{1p}$ and $\mathbf{E}_{1s}$ as well as $\mathbf{E}_{2p}$ and $\mathbf{E}_{2s}$. Other calculation details are similar to the above.

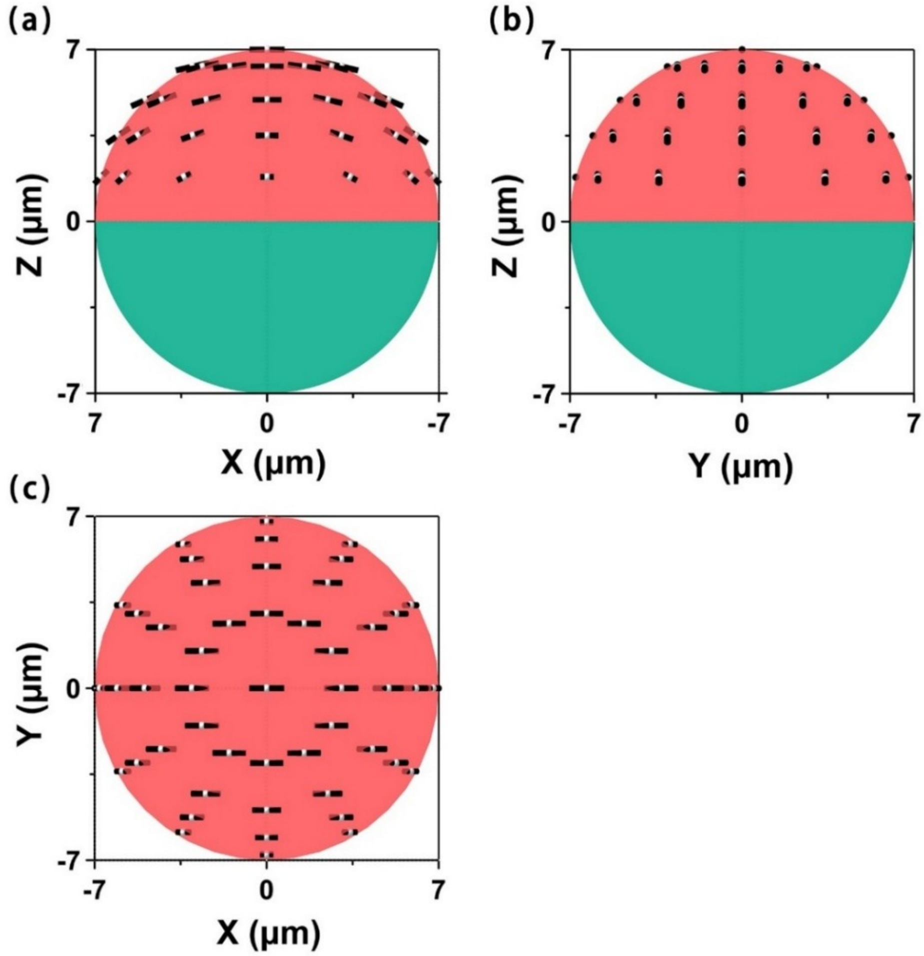

Fig. S9 Calculation results of the electric fields of the refracted light at different incident regions on the upper surface of the IAC-4 microspheres for the linearly polarized light irradiation. (a), (b) and (c) are respectively the front view, the side view and the top view of Fig. 5. The incident linearly polarized beam propagates along the negative z-axis with its electric vibration in x-axis direction. The amplitudes of the electric waves of the refracted light at each incident region (white dot) are represented as black line segments, which indicate both the vibration direction and relative amplitudes of the electric wave in the perspective view. The line segments in these three figures are projection drawings, whose lengths are proportional to the amplitude of the electric wave viewing with the specific perspective.

6. Photoinduced deformation of IAC-4 microspheres in high refractive index medium

In order to understand the effect of light refraction to the photoinduced deformation behavior and verify the theoretical calculations, the IAC-4 microspheres were immersed in a colorless aqueous solution of KSCN (66 wt%) and were irradiated by the linearly polarized laser beam (λ = 488 nm, I = 200 mW/cm^2) for a period of time (0.5 h and 1 h). The morphology of the microparticles was then characterized by SEM observation (Figure S10). Noteworthy, in this experiment, the silicon substrates loaded with microspheres were set in a flat petri dish containing the aqueous solutions, and they were both horizontally placed on the optical bench, rather than the vertical placement in Fig. S5. The horizontal or vertical placement did not affect the deformation process. As elucidated in the main text, the gravity shows no observable effect on the photoinduced deformation behavior of the IAC-4 microspheres.

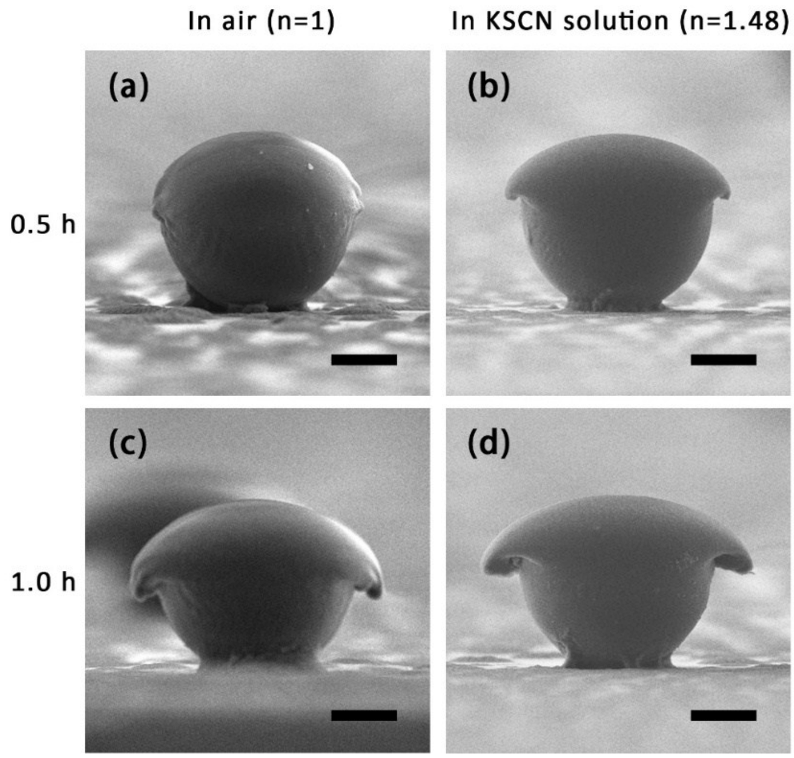

Fig. S10 Front view SEM images of the mushroom-like IAC-4 microparticles, after being irradiated with the linearly polarized light (λ = 488 nm, I = 200 mW/cm^2) for 0.5 h (a, b) and 1 h (c, d). The surrounding medium for the microspheres were the air (n = 1, a and c) and the aqueous solution of KSCN (66 wt%, n = 1.48, b and d), respectively. Scale bars are 5 μm.

As shown by the theoretical calculations (Fig. S11), due to the larger refractive index of the KSCN solution (n = 1.48, for λ = 488 nm) compared to the air (n = 1), the z-component of the electric field in the refracted light is reduced while its x-component increased. Accordingly, as shown in the front view SEM images (Fig. S10), the IAC-4 microspheres in the KSCN aqueous solution show more significant deformation along the x-axis compared to that in air, while their deformation toward the substrate (along the negative direction of z-axis) is relatively small. The agreement between the experimental result (Fig. S10) of the photoinduced deformation direction and the theoretical calculations about the electric field (Fig. S11) indicates that the light refraction plays a vital role to cause the observed complexity of the photoinduced deformation behavior of the ten-micron-sized IAC-4 microspheres.

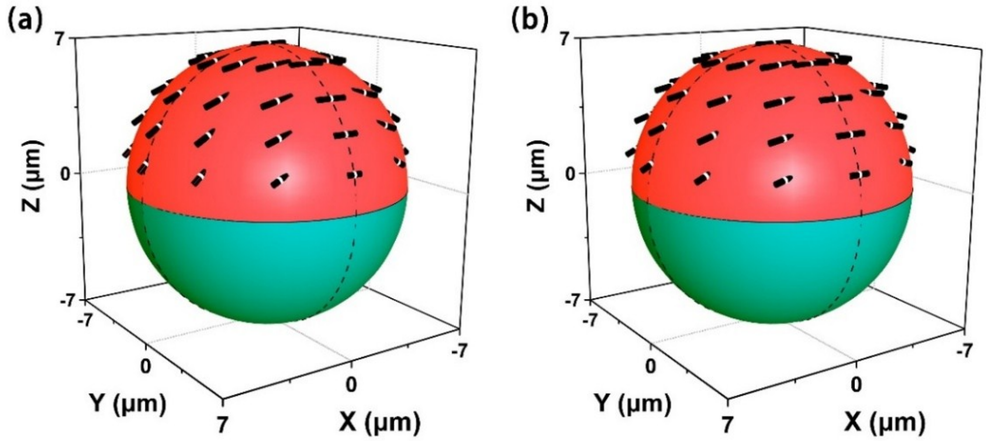

Fig. S11 Calculation results about the electric fields of the refracted light at different incident regions on the upper surface of the IAC-4 microspheres. The surrounding medium is respectively (a) the air (n = 1) and (b) the aqueous solution of KSCN (66 wt%, n = 1.48). The incident linearly polarized light propagates along the negative z-axis with its electric vibration in x-axis. The electric wave amplitudes of the refracted light at each incident region (white dot) are represented as black line segments, which indicate the vibration direction and relative amplitude of the electric field. In order to see clearly, some of the line segments are partially buried in the surface of the microsphere in the figure.

7. Calculated results of the circularly polarized light irradiation

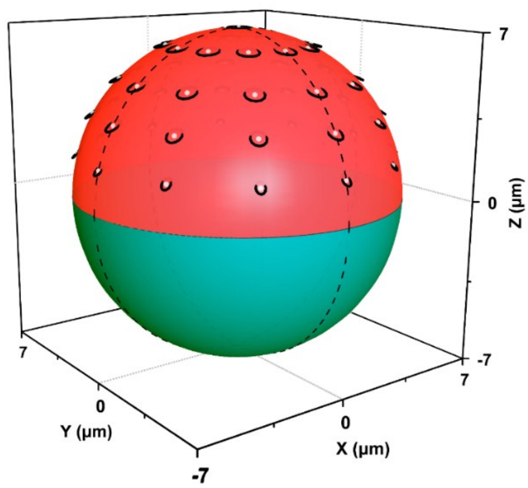

Fig. S12 Calculation results about the electric fields of the refracted light at different incident regions on the upper surface of the IAC-4 microsphere for the circularly polarized light irradiation. The incident circularly polarized beam propagates along the negative z-axis with its rotating electric field vector parallel to the xOy plane. The endpoints of the rotating electric field vector for the refracted light at each incident region (white dot) are connected by the black rings, which indicate the vibration plane and relative amplitudes of the electric field. Some of them are partially buried in the surface of the microsphere in the figure.

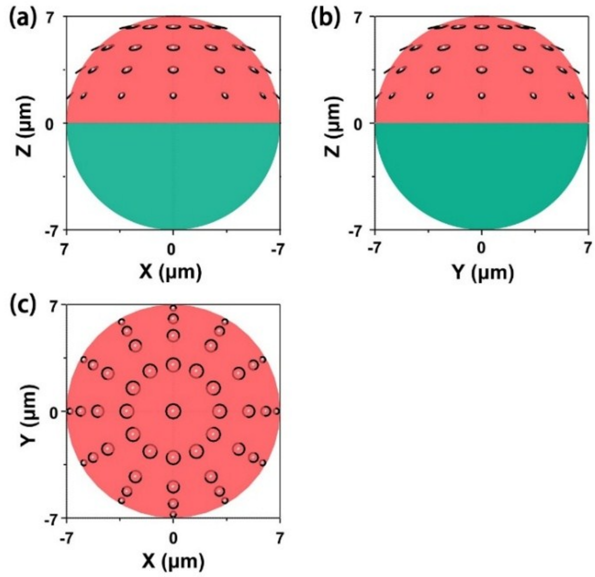

Fig. S13 Calculation results about the electric fields of the refracted light at different incident regions on the upper surface of the IAC-4 microsphere for the circularly polarized light irradiation. (a), (b) and (c) are respectively the front view, the side view and the top view of Fig. S12. The incident circularly polarized beam propagates along the negative z-axis with its rotating electric field vector parallel to the xOy plane. The endpoints of the rotating electric field vector for the refracted light at each incident region (white dot) are connected by the black rings, which indicate the vibration plane and relative amplitudes of the electric field. The black rings in these three figures are also projection drawings of Fig. S12 viewing with the specific perspective.

References

[S1] A. Lipson, S.G. Lipson and H. Lipson, Optical Physics. 4th ed., Cambridge University Press, Cambridge, 2011.